Co-solvent strategy for rechargeable post-lithium metal batteries

The potential increase in cost of lithium-ion batteries owing to the limited supply of lithium has prompted investigations into alternative and complementary rechargeable batteries that use post-lithium charge carriers with higher elemental abundance. However, achieving highly reversible post-lithium metal anodes with sufficient kinetics remains challenging. The addition of co-solvents to conventional electrolytes is emerging as an important strategy to resolve these issues. In this Perspective, we discuss the progress of the co-solvent strategy for sodium, potassium, magnesium, calcium, zinc and aluminium post-lithium metal batteries. The coordination ability of co-solvents with post-lithium charge carriers is presented as a useful guide for selecting co-solvents for the respective battery electrolytes, owing to its correlation with several influential factors that affect the electrochemical performance of the metal anodes, such as solvation structure, de-solvation process and solid electrolyte interphase formation. Additionally, a discussion is provided on the importance of unravelling the effects beyond the solvation sheath of cationic charge carriers and for the development of sustainable electrolytes.

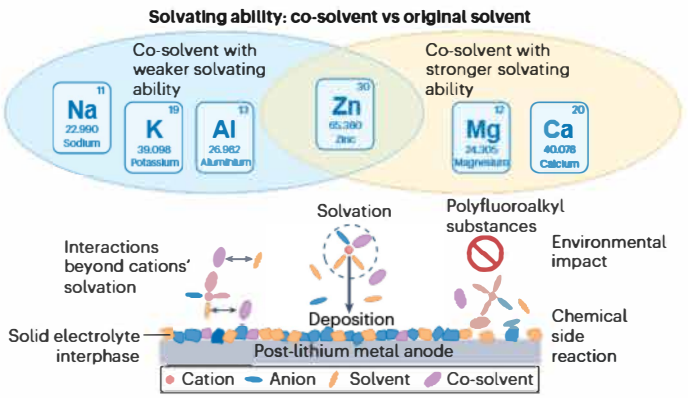

Introduction

The consideration of rechargeable batteries as convenient energy storage media plays crucial roles in our society, which is increasingly powered by renewable energy sources. The state-of-the-art battery technology, rocking-chair, lithium-ion batteries (LIBs), using graphite (372 mAh g^{-1}) anodes and transition-metal-based cathodes, has governed the market of portable electronics and is now rapidly penetrating the electric vehicle and stationary energy storage sectors[1]. However, the low abundance and uneven distribution of lithium resources and other critical materials (graphite, nickel and cobalt) have led to concerns over the future supply and rising cost to fulfil the vast demands of LIBs[2,3]. Consequently, efforts are underway to explore complementary and even alternative battery technologies using more sustainable elements (Table 1) as the charge carriers, known as post-lithium batteries[4,5]. By contrast, the replacement of Li^+ with alternative metal ions would weaken the energy density of the rocking-chair batteries where insertion-type negative electrode materials are used. The larger ionic radius and/or higher charge density of non-lithium metal cations affect the insertion kinetics and, therefore, reduce the specific capacity of the electrode materials[6]. Also, the redox potential of post-lithium couples is higher than that of Li/Li^+, which limits the possible output voltage of batteries[7]. In this context, adopting metal electrodes with high specific capacity (Table 1) and low redox potential is a viable protocol to enhance the energy density of post-lithium metal batteries[4,8,9]. For instance, Li et al.[10] reported a sodium metal battery with an energy density of more than 200 Wh kg^{-1} at the cell level, which is even higher than that of the commercial graphite||$LiFePO_4$ LIBs.

Achieving high reversibility of metal anodes is an essential requirement for practical high-energy-density and long-lifespan post-lithium metal batteries, which relates to not only anodes but also electrolytes[11–13]. The early exploration of electrolytes targeting highly reversible post-lithium metal anodes revealed the importance of optimizing the electrolyte solvation structure and its specific correlation with the resultant solid electrolyte interphase (SEI) and stripping and plating reversibility of the metal anode[14–18]. However, it was observed that the use of a sole solvent in these conventional electrolytes is insufficient to obtain the most functional solvation structure and a compromise of relevant electrolyte properties is a requisite, such as viscosity and ionic conductivity, which limits the cyclability and/or rate capability of the anodes and batteries[14,19–23]. The addition of co-solvents to these conventional electrolytes has emerged as an effective method to promote electrochemical performance through strengthening the solvation and/or compensating for compromised properties[24–29]. This co-solvent strategy facilitated the use of graphite anodes for the development of the current LIBs[30–32]. Therefore, this proposed approach — of considering the selection of co-solvents for the respective battery system — is expected to considerably boost the progress of post-lithium metal batteries.

In this Perspective, we present the advances of the co-solvent strategy in promoting the development of metal anodes for rechargeable post-lithium metal batteries. It has been shown that the solvation ability of the co-solvent with respect to the solvent in the original electrolytes provides valuable guidance for the primary co-solvent selection of different post-lithium metal anodes, as its correlation to various factors greatly affects the electrochemical performance of metal anodes, such as solvation structure, de-solvation processes and SEI formation. Moreover, for future electrolyte design of the post-lithium metal anodes, the importance of several aspects of co-solvent selection is emphasized, such as ion–solvent and solvent–solvent interactions beyond cation solvation, chemical side reactions at electrode surfaces and environmental impact.

Co-solvents for post-lithium alkali and aluminium metal anodes

For non-aqueous post-lithium alkali and aluminium metal batteries, coordination (or interactions) between the cationic charge carrier and anion is required to enable highly reversible metal anodes. As such, co-solvents exhibiting lower solvation ability towards the cationic charge carriers with respect to the original solvent of the conventional electrolytes, even non-solvating co-solvents, are adopted.

Sodium metal anodes

The electrolytes developed to enable highly reversible sodium metal anodes with stripping and plating Coulombic efficiencies (CEs) above 99.0% are mostly based on ether solvents. The optimal molar ratio of sodium salts versus solvating solvents (r) depends on the anion.

When sodium bis(fluorosulfonyl)imide (NaFSI) is used as the salt, a high salt concentration in the NaFSI/ether binary electrolytes is required, that is, a high r value. The increased salt concentration pushes the equilibrium between FSI^- and solvent in the Na^+ solvation sheath towards FSI^-, promoting the participation of additional FSI^- in forming an SEI that is more abundant in protective inorganic species[19,33]. As a consequence, sodium stripping and plating CEs higher than 99% can be reached in ether electrolytes with high NaFSI concentration, for example, 4 M equalling to $r = 0.625$ (refs. 19,34,35). However, the strengthened ion–ion and ion–solvent interactions in these high-concentration electrolytes (HCEs) reduce the fluidity and ion conductivity[19,33], limiting both the wettability of electrolytes towards the porous separator and electrodes and the rate capability of the cells. Subsequently, hydrofluoroethers with low viscosity, for example, bis(2,2,2-trifluoroethyl) ether, are introduced as co-solvents for the HCEs, and the newly obtained electrolytes are known as localized HCEs (LHCEs)[25,36–38], which are of use for lithium metal batteries[39,40]. The low viscosity of hydrofluoroethers decreases the viscosity of the HCEs, whereas it increases the ionic conductivity. Meanwhile, the fluorinated groups with strong electron-withdrawing effects considerably weaken the solvating ability of the molecules towards Na^+ and thus introduce a non-solvating character to the co-solvent, which preserves the local Na^+ solvation and anion-derived SEI in the native HCEs (Fig. 1a–c). Furthermore, it has been observed that these 'inert' co-solvents reduce not only the electrolyte resistance but also, more importantly, the interfacial resistance of sodium metal anodes[25,36]. As a result, LHCEs effectively promote the rate capability and reduce the polarization while maintaining the high CE (>99%) of sodium metal anodes. Nonetheless, the facilitated interfacial kinetics of the sodium metal anodes aided by co-solvents was not well understood. In 2022, Zhou et al.[41] revisited this gap in our understanding and conducted a comprehensive experimental and computational study of a similar LHCE. It was demonstrated that although hydrofluoroether co-solvents do not interact with Na^+, their interaction with 1,2-dimethoxyethane (DME) solvents reduces the concentration of DME and increases FSI^- in Na^+ solvation sheaths. This leads to the formation of an SEI with an abundance in the inorganic species derived from FSI^- and therefore reduces the energy barrier of Na^+ migration across the SEI for enhanced interfacial kinetics. In addition, highly fluorinated co-solvents are not always inert, with some of these species susceptible to defluorination reactions, resulting in the formation of metal fluorides in the inorganic-rich, protective SEI[42,43].

Table 1 | Abundance and properties of lithium with the most promising post-lithium candidates

Element (M)	Li	Na	K	Mg	Ca	Zn	Al
Relative atomic mass	6.94	22.99	39.10	24.31	40.08	65.38	26.98
Metal density (g cm^{-3})	0.53	0.97	0.86	1.74	1.55	7.14	2.70
Concentration in the Earth's crust (ppm)	20	28,300	25,900	20,900	36,300	75	81,300
Ionic charge carrier (M^{x+})	Li^+	Na^+	K^+	Mg^{2+}	Ca^{2+}	Zn^{2+}	Al^{3+}
Ionic radius (Å)	0.76	1.02	1.38	0.72	1.00	0.74	0.54
Ionic charge density (e $Å^{-3}$)	0.544	0.225	0.091	1.279	0.477	1.178	4.548
Redox potential of M/M^{x+} versus SHE (V)	−3.04	−2.71	−2.93	−2.36	−2.84	−0.76	−1.68
Gravimetric specific capacity (mAh g^{-1})	3,860	1,166	685	2,206	1,337	820	2,980
Volumetric specific capacity (mAh cm^{-3})	2,046	1,131	589	3,838	2,072	5,855	8,046

SHE, standard hydrogen electrode.

Unlike NaFSI, when sodium salts based on PF_6^- (refs. 15,44), BF_4^- (refs. 15,45), $SO_3CF_3^-$ (refs. 15,46) and bulky carborane[47] or tetraphenylborate[48] anions that do not preferentially coordinate to Na^+ are used to pair linear ethers, highly reversible sodium metal stripping and plating with CE of 99.5–99.9% and low polarization can already be achieved in conventional 1 M and even lower salt concentrations ($r < 0.2$) – that is, low concentration electrolytes[49]. Nonetheless, Na^+ solvation sheaths in these electrolytes contain a large amount of ether solvents particularly at low salt concentrations[50], whereas the sluggish de-solvation of strongly coordinating linear solvents at low temperatures results in dendritic growth and severe polarization of sodium metal anodes. To overcome this issue, cyclic ether solvents, such as 1,3-dioxolane and tetrahydrofuran, with relatively weaker solvation abilities than the linear ether solvents are used as co-solvents for these electrolytes[26,51–53]. Owing to their weaker solvation ability, the proportion of cyclic ethers entering Na^+ solvation sheaths is lower than that of linear ethers. As the overall salt concentration is unchanged, the use of a co-solvent decreases the amount of linear ether molecules in the Na^+ solvation sheaths and increases the proportion of anions coordinating to Na^+ (Fig. 1d). Owing to the electrostatic repulsion effect of negatively charged anodes on anions during sodium plating, the de-solvation barrier of the anion is negligible compared with solvents[54]. In addition, the de-solvation energy of weakly coordinated cyclic ethers is much lower than that of strongly coordinated linear ethers[51] (Fig. 1e). Therefore, the de-solvation kinetics is effectively promoted with cyclic co-solvents. Moreover, it has been reported that the increased number of anions in the Na^+ solvation sheath enriches the inorganic species of the SEI[26,51]. Consequently, these co-solvent-aided electrolytes enable high sodium stripping and plating CEs of up to 99.9% at −40 °C and stabilize the cycling of Na||Na cells even at −80 °C (refs. 26,52).

As LHCEs exhibit a similar anion-rich solvation of Na^+, they also enable the operation of sodium metal anodes at sub-zero temperatures[55]. Nonetheless, their generally lower ionic conductivity at low temperatures, compared with the electrolytes using linear and cyclic dual solvents, results in inferior low-temperature performance[26,52,55]. By contrast, the considerably reduced content of free solvating solvent molecules in LHCEs expands their potential compatibility with cathodes. Given that ether solvents are known for their poor anodic stability, LHCEs with a lower content of free solvating solvent molecules demonstrate improved anodic stability[36,45], allowing for the use of cathode materials with higher operation voltage. Additionally, the presence of the free solvating solvents increases the solubility of polysulfides in electrolytes, making LHCEs more commonly used for sodium-sulfur batteries[37,38,55].

Potassium metal anodes

Owing to the chemical similarity of sodium and potassium, both the mentioned electrolyte strategies for sodium metal anodes have been investigated for potassium metal anodes as well. Despite the extensive exploration on various salts and solvents, the CEs of potassium stripping and plating in electrolytes adopting solvating solvents solely and 1 M or lower salt concentration cannot attain 99% (refs. 56–59). Nonetheless, when a KFSI salt is paired with ether or phosphate ester solvents for HCEs, the CE of potassium metal anodes has been reported to exceed 99%, such as with 2 M KFSI in triethyl phosphate and $[KFSI]_{0.6}[DME]_1$ (with KFSI and DME in a molar ratio of 0.6:1)[60,61].

In this context, non-solvating and low-viscosity co-solvents are adopted for K^+-based HCEs, which is equally effective (as for the Na^+-based ones) in promoting fluidity, ionic conductivity and anode reversibility[24,62–64]. Nonetheless, the higher reactivity of potassium compared with sodium leads to some restrictions on the design of the LHCEs. Chen et al.[65] compared the compatibility of alkali metal anodes with ether-based LHCEs using DME as the solvent, FSI^- as the anion and 2,2,2-trifluoroethyl 1,1,2,2-tetrafluoroethyl ether as the co-solvent, displaying a previously unnoticed degradation mechanism in these systems. Specifically, the ether solvent reacts with these alkali metals to generate solvated electrons that attack the hydrofluoroether co-solvent (Fig. 2a). This degradation is limited for sodium and, in particular, lithium. However, this process severely hinders the formation of a stable SEI on potassium metal, leading to the continuous degradation of both electrolytes and potassium metal – although the CE of potassium stripping and plating can still reach 97.4%. This degradation is supported by the gas evolution (Fig. 2b) and colour change of the metal (Fig. 2c–e), which is accompanied with the reactions when the metal is stored in the LHCE. As shown in Fig. 2e, a piece of potassium metal immersed in the tested ether-based LHCEs fully corroded and formed black products. Nonetheless, this degradation occurs only when ether solvents are used. For instance, such degradation of potassium metal is not observed in carbonate ester-based or phosphate ester-based LHCEs, owing to the inability to generate solvated electrons in these ester solvents[65–67].

Developing LHCEs that do not rely on solvating ether solvents is a feasible approach to avoid this degradation, such as phosphate ester

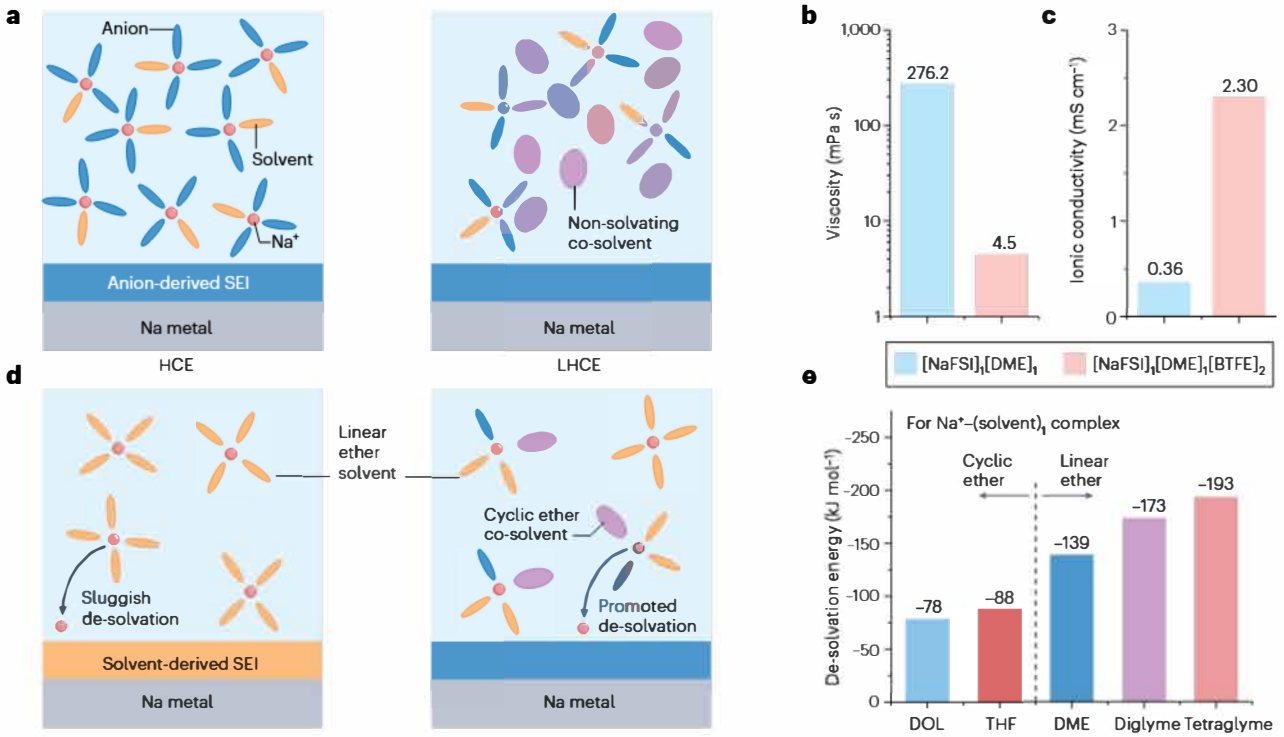

Fig. 1 | Co-solvent strategy for sodium metal anodes. a, Illustration of the dilution from a high-concentration electrolyte (HCE) to a localized high-concentration electrolyte (LHCE) via the addition of non-solvating co-solvents. In the LHCE, the non-solvating co-solvent not coordinating with Na^+ retains the initial solvation structure of Na^+ in the parental HCE as well as the anion-derived solid electrolyte interphase (SEI) on sodium metal anodes. Viscosity (part **b**) and ionic conductivity (part **c**) of $[NaFSI]_1[DME]_1$ (a typical HCE) and $[NaFSI]_1[DME]_1[BTFE]_2$ (a typical LHCE) at room temperature. NaFSI, DME and BTFE represent sodium bis(fluorosulfonyl)imide, 1,2-dimethoxyethane and bis(2,2,2-trifluoroethyl) ether, respectively. The co-solvent effectively decreases the viscosity and promotes the ionic conductivity. The data of parts **b** and **c** are from ref. 25. **d**, Illustration of the effect of cyclic ether co-solvents on the low-concentration electrolytes with linear ether solvents. With sodium salt concentration unchanged, cyclic ether co-solvents exhibiting weaker solvation ability with respect to the linear ether solvents decrease the amount of linear ether molecules in the Na^+ solvation sheaths and increase the proportion of anions coordinating to Na^+, which leads to anion-derived SEI and promoted the de-solvation process of Na^+ upon sodium deposition. **e**, De-solvation energy of Na^+–(solvent)$_1$ complexes with various linear and cyclic ethers. DOL and THF represent 1,3-dioxolane and tetrahydrofuran, respectively. The data of part **e** are from ref. 51.

solvents[66]. By contrast, the observed degradation does not mean that ether-based HCEs cannot be used in LHCE strategies. Instead, this suggests that a rational design of the electrolyte formulation and careful compatibility validation of the derived LHCEs towards potassium metal anodes is required. When non-solvating co-solvents that can tolerate the attack from the solvating electrons are used, and/or the derived SEI is sufficiently robust to isolate the potassium metal anode from contact with the electrolytes, this degradation can be terminated.

Aluminium metal anodes

The earliest electrolytes proposed for rechargeable aluminium metal batteries were inorganic chloroaluminate melts, such as the binary NaCl-$AlCl_3$ or the ternary KCl-NaCl-$AlCl_3$, which strip and plate aluminium metal via the conversion between $AlCl_4^-$ and $Al_2Cl_7^-$ (ref. 68) (equation (1)). However, the high melting points of these electrolytes (above 80 °C) limit their use at room temperature[69,70]. To fit the requirement of room-temperature applications, bulky organic ions (M^+), such as 1-ethyl-3-methylimidazolium cations ($Emim^+$), are used as alternatives to Na^+ and K^+ of the inorganic chloroaluminates, which effectively reduces the melting point to room temperature[71]. The obtained MCl-$AlCl_3$ binary electrolytes are considered as room-temperature ionic liquid electrolytes (ILEs). Subsequently, the high cost of the organic chloride (MCl) pushed the development of alternative low-cost, deep eutectic liquid-based electrolytes (DELEs) prepared via mixing $AlCl_3$ as a Lewis acid with a Lewis basic ligand, such as urea and acetamide, in which the heterolytic cleavage of $AlCl_3$ generates $AlCl_4^-$, $Al_2Cl_7^-$ and $[AlCl_2{\cdot}(ligand)_n]^+$ for stripping and plating[72–74], as described by equation (2):

$$4Al_2Cl_7^- + 3e^- \leftrightarrow Al + 7AlCl_4^-, \quad (1)$$

$$2[AlCl_2{\bullet}(ligand)_2]^+ + 3e^- \leftrightarrow Al + AlCl_4^- + 4(ligand). \quad (2)$$

ILEs and DELEs have been the most commonly used electrolytes for rechargeable aluminium metal batteries. However, the strong Coulomb force between the cations (M^+ and $[AlCl_2{\bullet}(ligand)_2]^+$) and anions ($Al_2Cl_7^-$ and $AlCl_4^-$) leads to high viscosity and limited ionic conductivity for ILEs and particularly DELEs[20]. Inspired by the strategy of LHCEs, non-solvating and low-viscosity 1,2-difluorobenzene (dFBn)

was reported as a co-solvent for ILEs and DELEs[27,75]. The addition of dFBn effectively promotes the fluidity and ionic conductivity. In particular, it does not change the relative intensity or position of the Raman peaks originating from $AlCl_4^-$ and $Al_2Cl_7^-$, which demonstrates that the solvation structure is maintained, as well as the equilibrium between these two species[27,75]. Therefore, the reversible stripping and plating of aluminium is attained with promoted overall kinetics. For example, $[AlCl_3]_{1.3}[Urea]_1$ exhibits a viscosity of 316 mPa s and an ionic conductivity of 0.5 mS cm^{-1} at room temperature, whereas these values for a diluted electrolyte, such as $[AlCl_3]_{1.3}[Urea]_1[dFBn]_{0.4}$, are 42.5 mP s and 1.95 mS cm^{-1}, respectively[27]. The polarization of Al||Al symmetric cells at 0.5 mA cm^{-2} decreases from 0.57 V to 0.2 V with the aid of co-solvents. The non-solvating and inert features of the co-solvent are important when selecting the co-solvent; otherwise, the change in the equilibrium of the chloroaluminates and the reaction between the co-solvent and the electrolytes would destroy the stripping and plating of aluminium metal. In fact, when dimethyl carbonate — a conventional solvating organic solvent for battery electrolytes — is used as the co-solvent for $[AlCl_3]_{1.3}[Urea]_1$, the obtained electrolyte does not allow the operation of Al||Al symmetric cells[27]. Moreover, it has been reported that the CE of aluminium stripping and plating is improved from ~80% for $[AlCl_3]_{1.3}[Urea]_1$ to 88% for $[AlCl_3]_{1.3}[Urea]_1[dFBn]_{0.4}$ (ref. 27). Although the reversibility of aluminium stripping and plating processes still needs to be improved, this result demonstrates the benefits of adding non-solvating co-solvents to the electrolytes for aluminium metal batteries.

Co-solvents for alkaline-earth metal anodes

For non-aqueous magnesium and calcium metal batteries, co-solvents exhibiting strong coordination ability to the divalent alkaline-earth cations are used for the more traditional electrolytes, to improve the kinetics and reversibility of the alkaline-earth metal anodes.

Magnesium metal anodes

Several chloride-based electrolytes have been reported to enable highly reversible magnesium stripping and plating with low polarization — electrolytes such as ethereal solutions of Grignard reagents (*R*Mg*X*, *R*: organic group; *X*: halogen ligand)[76], binary complex of MgR_2 and $AlCl_{3-n}R_n$ (*R*: alkyl group)[77] and 'all-phenyl' complex of PhMgCl (Ph: phenyl) and $AlCl_3$ (ref. 78). However, their limited electrochemical stability window and/or high corrosivity associated with the chloride initiated the investigation into chloride-free electrolytes[79].

Various conventional and commercial Mg^{2+}-based salts and solvents have been paired to prepare electrolytes for magnesium metal batteries[79]. Among them, electrolytes using magnesium bis(trifluoromethanesulfonimide) ($Mg(TFSI)_2$) salt and ether solvents, such as DME, are the few candidates that enable stripping and plating of

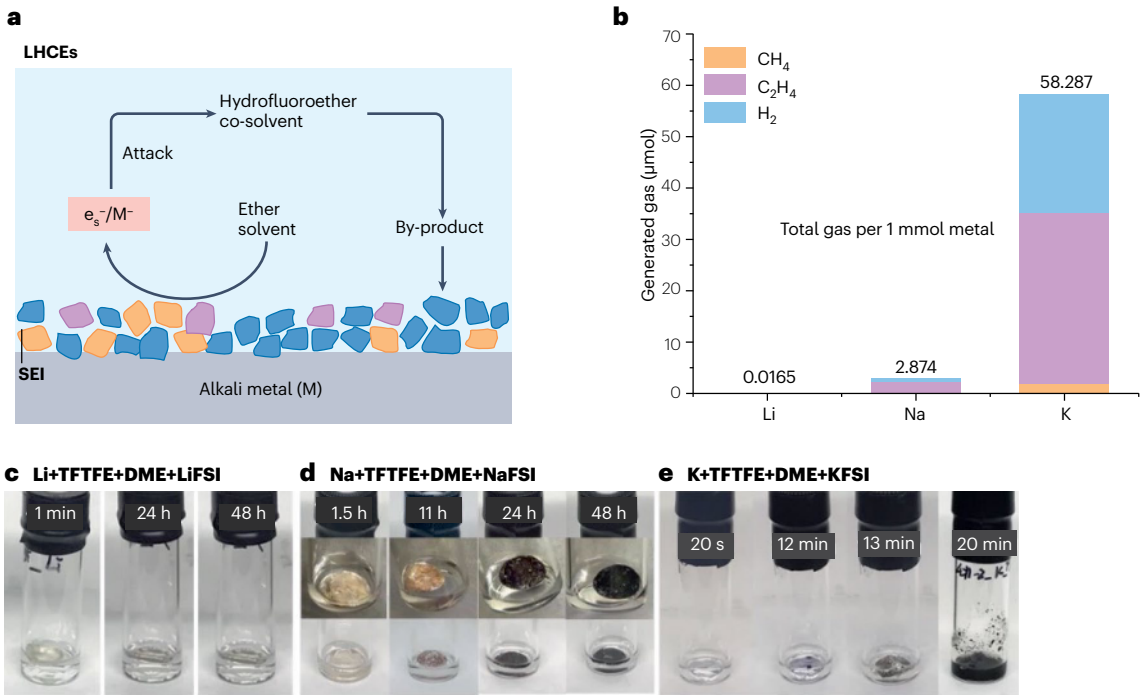

Fig. 2 | Solvated electron-based degradation of ether-based electrolytes and alkali metal anodes. a, Illustration of the degradation in ether-based localized high-concentration electrolytes (LHCEs). Owing to the lack of a sufficiently protective solid electrolyte interphase (SEI), the ether solvent reacts with alkali metals (M) to generate alkali metal cation (M^+) and solvated electrons (e^-/M^-). The latter attack the hydrofluoroether co-solvent and the generated by-product further deposits on the surface of alkali metal anodes, which hinders the formation of a stable SEI. **b**, Amount of gas generated per 1 mmol alkali metal immersed in the corresponding LHCEs. A higher amount of the gas indicates more severe degradation. Therefore, this degradation is much more severe for potassium, compared with sodium and especially lithium. The data of part **b** are from ref. 65. Photos of lithium (part **c**), sodium (part **d**) and potassium (part **e**) immersed in corresponding LHCEs using bis(fluorosulfonyl)imide (FSI^-)-based salts, 1,2-dimethoxyethane (DME) solvent and 2,2,2-trifluoroethyl 1,1,2,2-tetrafluoroethyl ether (TFTFE) co-solvent. Owing to the solvated electron-based degradation, potassium fully corroded and formed black products in 20 min. Sodium was also affected but the progress is much slower, and lithium maintained a silver-like surface, unchanged upon storage for 48 h. Parts **c**–**e** reprinted with permission from ref. 65, Wiley.

magnesium[16]. However, this process still suffers from low CE and high polarization in these types of electrolytes, which is caused by the decomposition of the electrolytes including both anions and solvents, and the derived thick passivation layer, that is, an SEI incapable of transporting Mg^{2+} (ref. 80). Computational studies have also confirmed that the ion pair, $[Mg^{2+}–TFSI^-]^+$, obtains one electron initially on the Mg^{2+} centre and forms the transient $[Mg^+–TFSI^-]$, which activates the decomposition of $TFSI^-$ and the formation of the passivation layer[21]. To resolve these issues, a family of methoxyethyl-amine co-solvents were used as co-solvents for the conventional $Mg(TFSI)_2$–DME binary electrolyte, for example, 2-methoxyethylamine (MOEA) and 1-methoxy-2-propylamine[29]. These co-solvents exhibit stronger coordination ability than DME and replace part of the DME in the solvation sheaths of Mg^{2+} (Fig. 3a). Compared with DME, the asymmetric co-solvents lead to a less compact and more polarizable Mg^{2+} solvation sheath, reducing the energy of the solvation reorganization for Mg^{2+} to accept electrons (Fig. 3b). Therefore, the reduction of Mg^{2+} to Mg is more favourable than the decomposition of solvent and anions in the solvation sheath, promoting the kinetics of magnesium deposition, and leads to the formation of a thinner SEI with fewer species from the electrolyte decomposition. As a result, the overpotential of Mg||Mg symmetric cells at 1.5 mA cm^{-2} decreases from above 2 V for blank electrolytes (0.5 M $Mg(TFSI)_2$ in DME) to lower than 0.1 V, and the CE of the Mg||stainless steel cells increases from 0% in the blank electrolyte to more than 99.5% (ref. 29). Inspired by this breakthrough, more electrolytes using commercially available salts and solvents for reversible magnesium metal anodes have been developed, accompanied with the insights from the role of the methoxyethyl-amine co-solvents[81–84].

Considering the high cost of $Mg(TFSI)_2$, some researchers have used the economical $Mg(SO_3CF_3)_2$ as the aforementioned ternary electrolytes[84,85]. Despite the replacement of $TFSI^-$ with $SO_3CF_3^-$, the methoxyethyl-amine co-solvents display similar effects on Mg^{2+} solvation regulation and on the kinetics, with CEs up to 99.3% of the magnesium metal anode[84,85]. More importantly, a relation between the solvation sheath and the SEI structure was revealed in electrolytes using $Mg(SO_3CF_3)_2$ as the salt, ethers as the solvents and MOEA as the co-solvent[84]. In the $Mg(SO_3CF_3)_2$–DME electrolyte, the high percentage of aggregate rich in $[Mg^{2+}–SO_3CF_3^-]^+$ induces the formation of inorganic MgF_2, MgO and $Mg(OH)_2$ in the inner layer of the SEI, whereas the ethereal solvents involved in contact–ion pair (in which one anion coordinates to one Mg^{2+}) and solvent-separated ion pair (in which Mg^{2+} does not directly interact with anions) decompose into organic species in the outer layer of the SEI. The inner SEI layer abundant with inorganic compounds prevents Mg^{2+} transport. As MOEA is added, MOEA involved in contact–ion pair and solvent-separated ion pair undergoes faster decomposition reactions than the ethereal solvents to produce organic N-containing species in the inner SEI, which – together with the decomposition of $SO_3CF_3^-$ in aggregate – leads to a concentration gradient of organic–inorganic species in the SEI. This effectively induces the transport of Mg^{2+}, thus reducing the overpotential and promotes the reversibility of magnesium metal anodes.

Apart from the methoxyethyl-amine co-solvents, other co-solvents have also been proposed for $Mg(TFSI)_2$–DME electrolytes, such as

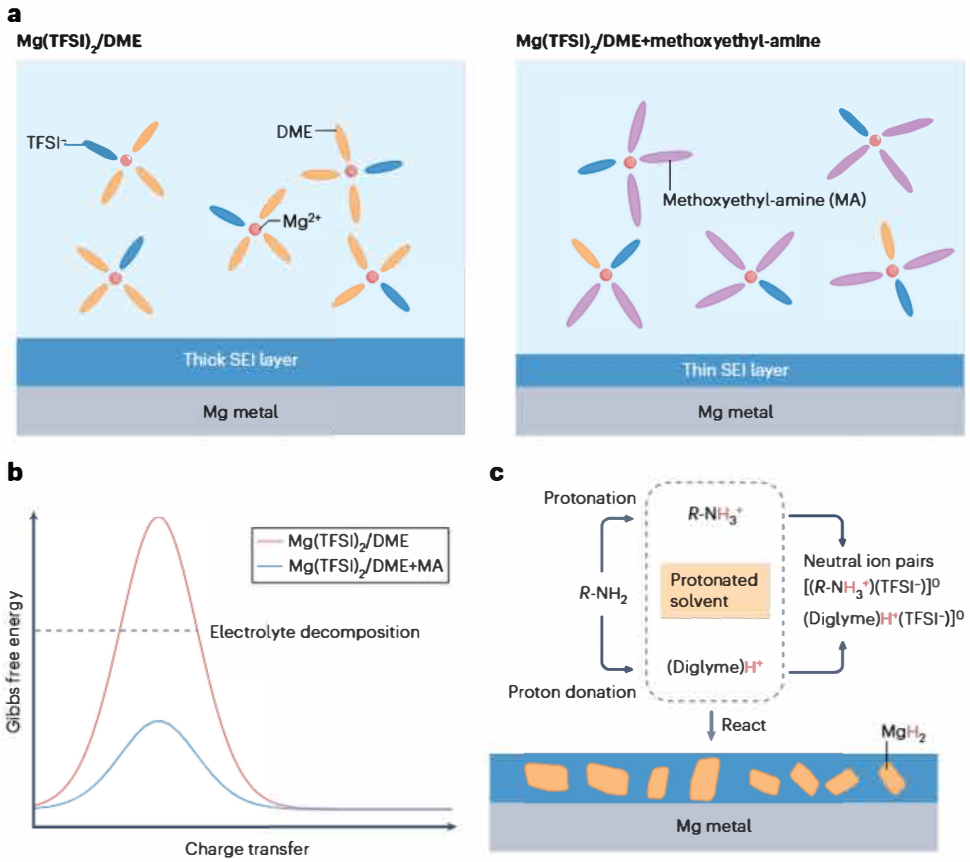

Fig. 3 | Illustration of the beneficial effect of co-solvents upon promoting the reversibility and kinetics of magnesium metal anodes. **a**, Illustration of the effect of methoxyethyl-amine (MA) co-solvent on the solvation structure of Mg^{2+} in $Mg(TFSI)_2$ and 1,2-dimethoxyethane (DME) electrolytes. DME and $Mg(TFSI)_2$ represent 1,2-dimethoxyethane and magnesium bis(trifluoromethanesulfonimide), respectively. Owing to the higher solvation ability with respect to DME, MA replaces part of DME in the solvation sheath of Mg^{2+}. **b**, Lower charge-transfer barrier mechanism: the presence of MA co-solvents reducing the energy barrier of solvent reorganization for Mg^{2+} to accept electrons, facilitating the facile reduction of Mg^{2+} to Mg instead of the electrolyte decomposing. **c**, Illustration of trace ionization of amine/ether co-solvents. The trace ionization of amine/ether leads to the formation of protonated solvents. These protonated species chemically associate with $TFSI^-$ to form naturally charged species, which mitigates the transport of $TFSI^-$ to electrode surface and its decomposition. Moreover, the protonated solvents promote the formation of protective MgH_2 species in the solid electrolyte interphase (SEI).

trimethyl phosphate (TMP) and amine[81,86,87]. As the phosphorus–oxygen bond with extreme electron richness competes with carbon–oxygen groups for the coordination with Mg^{2+}, TMP partially replaces the DME in Mg^{2+} solvation sheaths, which not only softens the solvation sheath deformation but also generates an SEI with increasing Mg^{2+} transport and electrical resistance[81]. With the addition of TMP co-solvent to the $Mg(TFSI)_2$–DME blank electrolyte, the overpotential of Mg||Mg cells at 0.1 mA cm^{-2} is decreased from over 2 V to around 0.15 V, and the ignorable CE of magnesium stripping and plating in $Mg(TFSI)_2$–DME is improved to 78% (ref. 81). Primary amines have been mentioned as the co-solvent for $Mg(TFSI)_2$-diglyme electrolytes, for example, 3-dimethylaminopropylamine (DMAPA or *R*-NH_2, *R*: $(CH_3)_2N(CH_2)_3$)[86]. Apart from the mechanism that is similar to the reorganization of Mg^{2+} solvation sheaths, a beneficial trace ionization of amine and ether co-solvents was proposed[86] (Fig. 3c), leading to the formation of protonated DMAPA (R-NH_3^+) and diglyme ((diglyme)H^+) generated through the intermolecular hydrogen exchange of DMAPA–DMAPA and DMAPA–diglyme. These protonated compounds can chemically associate with $TFSI^-$ to form neutrally charged species, which mitigates the decomposition of $TFSI^-$ on magnesium metal anodes as these neutral charged species are more difficult to transport to the surface of magnesium metal anodes under the electric field during charging and discharging with respect to the $[Mg^{2+}–TFSI^-]^+$ ion pairs. Moreover, the protonated DMAPA and diglyme can release active hydrogen species, facilitating the formation of protective MgH_2 species in the SEI. The effect of this trace ionization of amine or ether co-solvents has been further verified with a few primary, secondary and tertiary amines as the co-solvent for $Mg(TFSI)_2$–diglyme electrolytes. Owing to the highest ionization degree, the primary amines lead to the lowest overpotential (0.14 V) and best CEs (>90%) of Mg||Cu cells. The tertiary amines without a transferable proton improve neither the kinetics nor the CE. It was observed that methoxyethyl-amine co-solvents also contain primary amine groups. Hence, the trace ionization should also occur in electrolytes using methoxyethyl-amine co-solvents and contribute to the enhanced electrochemical performance of magnesium metal anodes.

Calcium metal anodes

Early exploration of calcium metal in conventional organic electrolytes revealed that the electrochemical behaviour is surface-film-controlled, which is similar to that of lithium, but the poor mobility of Ca^{2+} in the SEI blocks the deposition of calcium metal[88]. The investigation of electrolytes for calcium metal anodes was revitalized by the report of calcium metal stripping and plating in 0.45 M $Ca(BF_4)_2$ in a mixture of ethylene carbonate and propylene carbonate[89]. Despite the limited CE and high operation temperature (100 °C), this work demonstrated the feasibility of calcium stripping and plating using rationally optimized electrolytes. Several electrolytes have since been reported to enable stripping and plating of calcium metal at room temperature, including those based on BH_4^- (ref. 90), alkoxy-functionalized ionic liquids as solvents[18] and/or bulky carborane[91] or fluorinated alkoxyborate anions[23,92] such as tetrakis(hexafluoroisopropyloxy)borate anion ($[B(hfip)_4]^-$)[23,92]. It is worth noting that both the strategies of using the alkoxy-functionalized ionic liquids and the bulky anions are designed to decrease the number of anions in the solvation shell of Ca^{2+}. The alkoxy group with strong coordination ability is tethered to the organic cations of the ionic liquids, enabling the coordination of the organic cations towards Ca^{2+} and thus decreasing the $TFSI^-$ in Ca^{2+} solvation. The delocalized negative charge and large size of the carborane or fluorinated alkoxyborate anions lead to a weak interaction with Ca^{2+}, thereby making Ca^{2+} preferentially coordinate to the solvent rather than the anions. Hou et al.[93] revealed the correlation between the solvation of Ca^{2+} and the SEI for reversible calcium metal anodes. The anion in the solvation of Ca^{2+} leads to the formation of impermeable SEIs rich in inorganic species, such as CaF_2 and $CaCO_3$, whereas the solvent-dominated solvation structure results in organic-rich and inorganic-poor SEIs, facilitating Ca^{2+} transport for reversible calcium stripping and plating[93]. Therefore, the strategies promoting the formation of a solvent-rich solvation of Ca^{2+} are capable of reversible calcium stripping and plating at room temperature. By contrast, CEs ranging from 30% to 92% require improvement, which could be attributed to the insufficient coordination of the solvent towards Ca^{2+} (refs. 18,23,90–92).

In this context, co-solvents with strong solvating ability towards Ca^{2+} would be beneficial for the electrochemical performance of calcium metal anodes. Following the successful application for magnesium metal anodes, methoxyethyl-amine co-solvents with strong coordination ability towards metal cations have also been used for Ca^{2+}-based electrolytes[29]. Owing to the similar effect for magnesium metal anodes, adding 4-methoxybutan-2-amine co-solvent to 0.5 M $Ca[B(hfip)_4]_2$ in DME effectively improves the CE from ~80% to 96% (ref. 29). Dissolving 0.5 M $Ca(TFSI)_2$ in a 1:1 volume mixture of ionic liquid $EmimBF_4$ and dimethyl sulfoxide (DMSO) is designed for room-temperature rechargeable Ca-oxygen batteries[94]. Owing to its lower viscosity with respect to ionic liquid electrolytes and strong solvation towards Ca^{2+}, the addition of DMSO not only reduces the viscosity and improves the ionic conductivity but also decreases the coordination between the anions and Ca^{2+}. As a result, the CE of calcium stripping and plating is improved from ~11% to ~92%. Although further investigation is necessary, these results have shown that using co-solvents with strong solvating ability to adjust the solvation sheath of Ca^{2+} is an effective tool for promoting the reversibility of calcium metal anodes[29,94].

Co-solvents of aqueous electrolytes for zinc metal anodes

Owing to the high redox potential of zinc metal anodes (Table 1), zinc metal batteries struggle to compete with other metal batteries requiring non-aqueous electrolytes in terms of energy density. By contrast, this character, together with a high hydrogen evolution overpotential, makes zinc metal the only candidate in Table 1 to be reversibly stripped and deposited in aqueous electrolytes[95]. Compared with conventional anode materials for aqueous ion batteries, such as $LiTi_2(PO_4)_3$ (~130 mAh g^{-1} and −0.72 V versus a standard hydrogen electrode (SHE)) and $NaTi_2(PO_4)_3$ (~110 mAh g^{-1} and −0.82 V versus SHE)[96,97], zinc metal is garnering interest with a comparable redox potential of −0.76 V versus SHE and higher specific capacities of 840 mAh g^{-1} and 5,854 mAh cm^{-3}. Various neutral or mildly acidic aqueous electrolytes using commercially available zinc salts can facilitate reversible stripping and plating of zinc at conventional salt concentrations of ~1–2 M, but the notorious corrosion of zinc metal by H^+/H_2O and electrochemical reduction of H^+/H_2O remain, limiting the CE and long-term stability of zinc metal anodes[98]. Introducing organic co-solvents to aqueous Zn^{2+}-based electrolytes has proven effective in suppressing these side reactions and promoting the CE of zinc metal anodes to up to 99.8% (refs. 28,99–103), which benefits from the effects of electrolyte bulk and an electrolyte/zinc metal electrode interface.

Solvation and hydrogen bond reorganization

The addition of organic co-solvent to aqueous Zn^{2+}-based electrolytes exerts two effects in the electrolyte bulk: reorganizing the solvation

and hydrogen bond network, both of which can lower the activity of H_2O; and to promote the reversibility of zinc metal anodes.

Reducing H_2O in Zn^{2+} solvation sheath is initially considered to limit the activity of H_2O, and both high-polarity co-solvents with strong coordination ability and low-polarity co-solvents with weak coordination ability have been reported to achieve these effects[28,102,104] (Fig. 4a–c). For instance, high-polarity formamide is reported as a low-cost co-solvent for aqueous zinc acetate ($Zn(OAc)_2$) electrolytes[28]. Compared with H_2O, formamide possessing a higher dielectric constant (111 versus 80, respectively) has a stronger coordination with Zn^{2+}, thus replacing H_2O in the Zn^{2+} solvation sheath. The low dielectric constant of DME (6.9) is also considered as an organic co-solvent to modify the Zn^{2+} solvation sheath in aqueous electrolytes[102]. Considering 1 M $Zn(SO_3CF_3)_2$ in a H_2O and DME solvent and when the molar fraction of DME in the solvent is lower than 0.15, the DME is not involved in the inner solvation sheath of Zn^{2+}, owing to its relatively weaker solvation ability compared with H_2O towards Zn^{2+}. Nonetheless, the addition of DME pushes $SO_3CF_3^-$ anions into the solvation sheath of Zn^{2+}, thus reducing H_2O coordinated to Zn^{2+}.

The added organic solvents mostly contain one or more groups acting as a hydrogen bond acceptor and therefore can attract free H_2O via the formation of hydrogen bonds (Fig. 4d), such as the -OH groups in alcohols[105], $-SO_2-$ in sulfones[106], -SO- in sulfoxide[107], -CN in nitriles[108], -O- in ethers[102], $-CO_3-$ in carbonate esters[22], -CO- in amides[28], among others. The consequent interruption of the original hydrogen-bonded network in aqueous electrolytes suppresses the reduction of hydrogen involved in the network, which helps to increase the hydrogen evolution overpotential, decreases interfacial side reactions and promotes reversibility of zinc metal anodes[28,102,103,105,107,108]. In addition to a homogeneous distribution of organic solvents in the hydrogen-bonded network, a unique 'reverse micelle' core–shell architecture was uncovered in 3 M $Zn(SO_3CF_3)_2$ in $[H_2O]_4$[sulfolane]$_1$ – in which free H_2O with its hydrogen-bonded network is segregated into nanodomains by sulfolane[106]. The added sulfolane preferentially coordinates to Zn^{2+}; however, when the coordination of Zn^{2+} tends towards saturation with the increasing of sulfolane, the extra sulfolane coordinates with H_2O. The hydrophilic group (O = S = O) in sulfolane interacts with the H atoms in H_2O, whereas the hydrophobic alkane ring of the sulfolane assembles outside the nanodomains. As the Zn^{2+} coordinated by sulfolane is located outside the nanodomains, the reverse micelle structure does not block the transport of Zn^{2+} – but it limits H_2O and proton transport – which effectively suppresses the side reactions on the electrode surface.

Interfacial adsorption and the SEI

In addition to the electrolyte bulk, the beneficial effect of the organic co-solvents on the interface between electrolytes and zinc metal anodes has received increasing attention.

Some of the co-solvents exhibiting higher adsorption energy than H_2O on zinc metal anodes are reported to be preferentially adsorbed on these anodes, such as DMSO[107], acetone[109], *N*,*N*-dimethyl acetamide[110], *N*-methylacetamide[111] and TMP[112], which leads to an organic co-solvent adsorption layer on the zinc metal anode, that is, an inner Helmholtz layer that is rich in organic co-solvent molecules (Fig. 4e). Owing to the

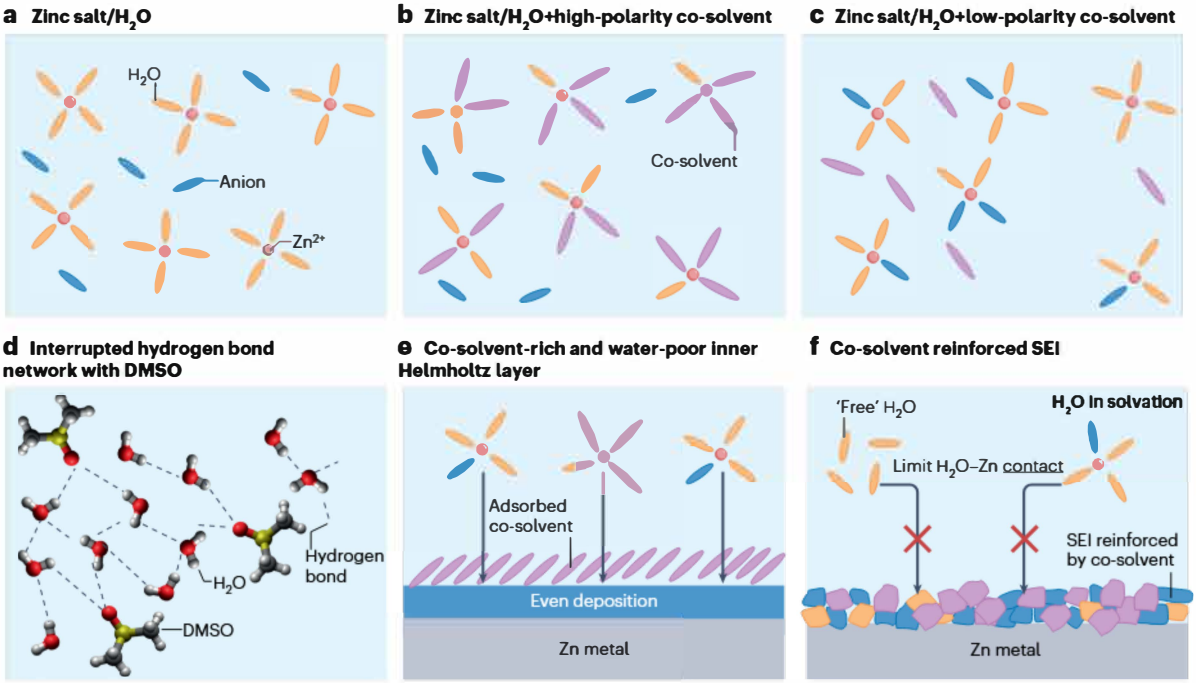

Fig. 4 | Illustration of the beneficial effects of co-solvent on the electrolyte bulk and an electrolyte–zinc metal electrode interface for promoted reversibility of zinc metal anodes. Illustration of the solvation sheath of Zn^{2+} in electrolytes using neat water solvent (part **a**), water and high-polarity co-solvent (part **b**) and water and low-polarity co-solvent (part **c**), respectively. The high-polarity co-solvent exhibiting strong coordination ability replaces part of H_2O in the solvation of Zn^{2+}. The low-polarity co-solvent has limited coordination with Zn^{2+} but promotes anions to replace part of H_2O in the solvation of Zn^{2+}. **d**, Illustration of an interrupted hydrogen-bonded network with the addition of organic solvents, such as dimethyl sulfoxide (DMSO). Illustration of the effect of organic co-solvents on the electrolyte–zinc metal anode interface: construction of a co-solvent-rich and water-poor inner Helmholtz layer owing to the adsorbed co-solvent (part **e**) and reinforced solid electrolyte interphase (SEI) by co-solvent addition (part **f**).

lack of H_2O in the inner Helmholtz layer, the side reaction requiring H_2O to participate is suppressed[109,111,112]. Moreover, the generated inner Helmholtz layer consisting of organic solvent promotes the wettability of the electrolyte towards zinc metal anodes, which is beneficial for an even nucleation during zinc deposition[22,108–110]. Apart from experimental tests of the contact angle and double layer capacitance to support the presence of the layer, Miao et al.[22] used molecular dynamic simulations to characterize the interface between zinc metal anodes and 2 M $Zn(SO_3CF_3)_2$ in H_2O electrolytes with or without 7 M diethyl carbonate (DEC), demonstrating that a hydrophobic DEC layer in close proximity to zinc metal anodes enables the formation of a H_2O-poor electrical double layer blocking water from contacting the Zn anode. It has also been reported that in the electrolytes of 1 M $Zn(OAc)_2$ in formamide/H_2O (1:1 in volume) and 2 M $ZnSO_4$ in DMSO/H_2O (2:8 in volume), the preferential adsorption of the organic co-solvents with respect to H_2O on the (002) plane of zinc metal leads to the (002) preferential orientation of zinc deposition upon repeated deposition of zinc. This results in a dense and smooth zinc morphology, in contrast to the porous and dendritic morphology observed when neat aqueous electrolytes are used[28,107].

The electrochemical and/or chemical reduction of anions, H_2O and organic co-solvent – as well as the consequent chemical reaction – at the interface of electrolytes and zinc metal anodes leads to the formation of an SEI on the anodes. The reduced activity of H_2O at the interface (owing to the organic co-solvent) limits the growth of the porous layer of basic zinc salts derived from H_2O decomposition, such as $Zn_4SO_4(OH)_6$ (refs. 99,111,112). Meanwhile, the absence of the bulky and irregular basic zinc salts allows the species derived from anions and organic co-solvents to form a dense and thin SEI, composed of components such as ZnF_2, $ZnCO_3$, ZnO, $Zn_3(PO_4)_2$, ZnP_2O_6 and various organic species[99,113,114]. In turn, this SEI effectively protects zinc metal anodes from direct contact with the electrolytes and inhibits further side reactions (Fig. 4f). Several of the SEI component species exhibit Zn^{2+} transport, but not that of electrons[115]. Liu et al.[113] compared pre-cycled and bare zinc metal electrodes in a 0.5 M $ZnSO_4$ aqueous electrolyte. The zinc metal electrodes that were previously cycled in a phosphonate-based non-aqueous electrolyte exhibit a monolithic phosphate SEI. Such an SEI leads to considerably longer lifespans compared with bare Zn electrodes undergoing repeated stripping and plating in the aqueous electrolyte (800 h versus ~70 h), which verifies the positive effect of the SEI on the reversibility of zinc metal anodes[113]. Also, the addition of propylene carbonate as co-solvent to $Zn(SO_3CF_3)_2$ aqueous electrolytes resulted in a hydrophobic surface of the zinc metal anodes owing to the formation of a hydrophobic SEI upon cycling, which further prohibits side reaction between Zn and water[100].

Overlaying multiple effects

The co-solvent introduced to the aqueous electrolyte for zinc metal batteries typically provides multiple beneficial effects, ameliorating the CE of zinc stripping and plating and prolonging the cycle life. For instance, DME as the co-solvent added to a 1 M aqueous $Zn(SO_3CF_3)_2$ electrolyte modifies the solvation sheath of Zn^{2+}, the hydrogen-bonded network and the SEI[102]. The former two aspects suppress the hydrogen evolution originating from the coordinated and 'free' water. Nonetheless, there are still plenty of water molecules in the solvation sheath and hydrogen-bonded network that can participate in hydrogen evolution reactions when the water is in contact with the zinc anodes. At the interface of the electrolyte and anode, the anion-rich solvation of Zn^{2+} leads to the formation of a protective SEI rich in inorganic species (such as ZnF_2), which in turn limits the hydrogen evolution reaction. Benefiting from the synergy of these effects, the average CE of Zn||Cu cells can be improved from 99.3% for 1 M $Zn(SO_3CF_3)_2$ in H_2O to 99.8% for 1 M $Zn(SO_3CF_3)_2$ in $[H_2O]_{0.85}[DME]_{0.15}$.

In addition to these favourable effects, the negative impact of organic co-solvents on the ionic conductivity and viscosity of these aqueous electrolytes should be considered when optimizing the co-solvent content. The original aqueous electrolytes with a zinc salt concentration of ~1–2 M usually exhibit an ionic conductivity of up to 50 mS cm^{-1} and viscosity <5 mPa s at room temperature[101,110,116]. The addition of organic co-solvent typically decreases ionic conductivity and increases viscosity[101,110,116,117]. Nonetheless, when water constitutes the major solvent (for example, >50 vol%), the electrolytes can still have a viscosity below 10 mPa s and ionic conductivity above 10 mS cm^{-1}, meeting the requirements for battery applications[101,110,116].

Discussion and outlook

The advances in electrolyte design confirm that the addition of co-solvents to conventional electrolytes is an effective strategy for enhancing the kinetics and/or reversibility of post-lithium metal anodes in high-performance batteries. The solvation ability of the co-solvent with respect to the solvent in the original electrolytes provides valuable guidance for the primary co-solvent selection for different post-lithium metal anodes. For instance, the electrolytes for post-lithium alkali and aluminium metal anodes require co-solvents, exhibiting lower solvation ability towards the cationic charge carriers to preserve and even strengthen the original cationic charge carriers' anion-rich solvation. In this context, the strongly solvating co-solvents entering the cationic charge carriers' solvation structure to improve the kinetics and reversibility of alkaline-earth metal anodes are not suitable for alkali and aluminium metal anodes.

This guidance is based on the effect of a co-solvent on the solvation structure and the correlation among the solvation structure, de-solvation processes and SEI formation. Therefore, further investigation into these relationships would clarify the influence of these factors for rationally designing electrolytes. For example, the relationship between the solvation ability and molecular structure of organic solvents is the cornerstone for designing co-solvents to adjust the equilibrium between anions and organic solvents in the solvation sheath. It should be noted that although the order of solvent coordination ability for a certain metal cation can yield useful insights for other cations when selecting co-solvents, the characteristics of the metal cation also influence its coordination with the solvent. For instance, DME has a strong coordination ability towards Zn^{2+} but much weaker coordination with Ca^{2+}, as Ca^{2+} has a larger ionic radius (Table 1), resulting in a less favourable geometry for coordination with the short DME molecules[118]. The dynamic process of de-solvation and the accompanying decomposition of solvation components for SEI formation need to be examined to identify the most effective solvation structure for better information on electrolyte design. This is particularly important for systems in which the role of the SEI is still unclear, such as aluminium, magnesium and calcium. Investigating ion mobility and electronic and mechanical properties of the commonly observed SEI components is also crucial for the rational design of electrolytes and to optimize the interphase.

Apart from cation solvation, there are other ion–solvent and solvent–solvent interactions present in the electrolytes that can affect the electrochemical performance. These functional interactions affect the fluidity and ionic transport of the electrolytes, as well as the solubility of co-solvents in the parent electrolyte. The interactions beyond the solvation of cations can also influence the solvation sheath of

the cationic charge carriers. For example, it was confirmed that the interaction between a hydrofluoroether co-solvent and an ether solvent in LHCEs led to more anions participating in the solvation sheath of cations[119]. Moreover, these components could decompose when they are in contact with electrodes, contributing to SEI formation and affecting the reversibility of metal anodes. For magnesium metal batteries, the trace ionization of amine-ether co-solvents affects the mobility and decomposition of $TFSI^-$, as well as the formation of MgH_2 species in the SEI. The reorganized hydrogen-bonded network, with the addition of organic co-solvent in aqueous electrolytes, also affects the hydrogen evolution reaction of the electrolyte on zinc metal anodes. Nevertheless, these interactions have received less focus with respect to the solvation of cations. Further research on how to modulate these interactions through electrolyte design and how such interactions influence functionality is anticipated to ameliorate the electrochemical performance of post-lithium metal anodes.

The chemical side reaction at the electrolyte and metal anode interface is also of relevance, particularly in systems already exhibiting extremely high CEs for more practical applications, such as sodium and zinc. The degradation of metal anodes owing to these side reactions is considered for the CE obtained with electrochemical tests, but a single stripping and plating cycle of the CE test in the reported literature usually takes a few hours, which could mask existing chemical degradation of the active metal in the anodes. For instance, the CE of potassium stripping and plating in the ether-based LHCE with severe chemical corrosion can still reach 97.4% (ref. 65). Although an elevated CE approaching 99.8% has been reported for Na and Zn (refs. 26,99), chemical degradation of the metal and electrolyte might still persist. In practical use, the metal anode in the cells needs to be compatible with electrolytes for operation over longer time durations such as months and even years. The consumption of the active metal, as well as the electrolytes, during the long service time will lead to a considerable negative impact on the cyclability of the batteries. In this context, stability tests and the study of the degradation mechanism of the post-lithium metal anode in the electrolyte during the shelf life will optimize the electrolytes for practical applications.

In addition, the environmental impact of the electrolytes should be considered. The majority of the non-solvating co-solvents of LHCEs for sodium-based, potassium-based and aluminium-based batteries, as well as most anions for magnesium and calcium batteries, and some anions for zinc batteries are harmful perfluoroalkyl and polyfluoroalkyl substances (PFAS) — that is, they contain $-CF_2-$ and/or $-CF_3$ groups, leading to environmental and occupational safety concerns. Restrictions on the use of PFAS are being introduced worldwide, for example, a proposal restricting the manufacture, placement on the market and use of PFAS in the European Union was submitted in 2023 by authorities in Denmark, Germany, the Netherlands, Norway and Sweden to the European Chemical Agency. Moreover, the high content of fluorine leads to increasing costs. As a result, a few PFAS-free and even fluorine-free non-solvating co-solvents have been applied to LHCEs for lithium metal batteries, and these electrolytes could be promising candidates for applications in post-lithium metal batteries[120–123]. Therefore, apart from the use of these substances to enhance performance, specific steps are required to develop PFAS-free and even fluorine-free non-solvating co-solvents to reduce the reliance on PFAS-based salts and to ultimately realize PFAS-free electrolytes for sustainable post-lithium metal batteries.

References

1. Tian, Y. et al. Promises and challenges of next-generation 'beyond Li-ion' batteries for electric vehicles and grid decarbonization. *Chem. Rev.* **121**, 1623–1669 (2021).
2. Vaalma, C., Buchholz, D., Weil, M. & Passerini, S. A cost and resource analysis of sodium-ion batteries. *Nat. Rev. Mater.* **3**, 18013 (2018).
3. Ji, H., Wang, J., Ma, J., Cheng, H. M. & Zhou, G. Fundamentals, status and challenges of direct recycling technologies for lithium ion batteries. *Chem. Soc. Rev.* **52**, 8194–8244 (2023).
4. Canepa, P. et al. Odyssey of multivalent cathode materials: open questions and future challenges. *Chem. Rev.* **117**, 4287–4341 (2017).
5. Gao, Y., Yu, Q., Yang, H., Zhang, J. & Wang, W. The enormous potential of sodium/potassium-ion batteries as the mainstream energy storage technology for large-scale commercial applications. *Adv. Mater.* **36**, e2405989 (2024).
6. Gautam, G. S. et al. First-principles evaluation of multi-valent cation insertion into orthorhombic V_2O_5. *Chem. Commun.* **51**, 13619–13622 (2015).
7. Innocenti, A., Beringer, S. & Passerini, S. Cost and performance analysis as a valuable tool for battery material research. *Nat. Rev. Mater.* **9**, 347–357 (2024).
8. Wang, X. et al. Building stable anodes for high-rate Na-metal batteries. *Adv. Mater.* **36**, 2311256 (2024).
9. Lei, Y. J. et al. Progress and prospects of emerging potassium–sulfur batteries. *Adv. Energy Mater.* **12**, 2202523 (2022).
10. Li, Y. et al. Interfacial engineering to achieve an energy density of over 200 $Wh\,kg^{-1}$ in sodium batteries. *Nat. Energy* **7**, 511–519 (2022).
11. Hobold, G. M. et al. Moving beyond 99.9% Coulombic efficiency for lithium anodes in liquid electrolytes. *Nat. Energy* **6**, 951–960 (2021).
12. Li, M. et al. Design strategies for nonaqueous multivalent-ion and monovalent-ion battery anodes. *Nat. Rev. Mater.* **5**, 276–294 (2020).
13. Wu, W., Luo, W. & Huang, Y. Less is more: a perspective on thinning lithium metal towards high-energy-density rechargeable lithium batteries. *Chem. Soc. Rev.* **52**, 2553–2572 (2023).
14. Yamada, Y. & Yamada, A. Review — superconcentrated electrolytes for lithium batteries. *J. Electrochem. Soc.* **162**, A2406–A2423 (2015).
15. Le, P. M. L. et al. Excellent cycling stability of sodium anode enabled by a stable solid electrolyte interphase formed in ether-based electrolytes. *Adv. Funct. Mater.* **30**, 2001151 (2020).
16. Ha, S. Y. et al. Magnesium(II) bis(trifluoromethane sulfonyl) imide-based electrolytes with wide electrochemical windows for rechargeable magnesium batteries. *ACS Appl. Mater. Interfaces* **6**, 4063–4073 (2014).
17. Zhang, N. et al. Cation-deficient spinel $ZnMn_2O_4$ cathode in $Zn(CF_3SO_3)_2$ electrolyte for rechargeable aqueous Zn-ion battery. *J. Am. Chem. Soc.* **138**, 12894–12901 (2016).
18. Gao, X. et al. Alkoxy-functionalized ionic liquid electrolytes: understanding ionic coordination of calcium ion speciation for the rational design of calcium electrolytes. *Energy Environ. Sci.* **13**, 2559–2569 (2020).
19. Lee, J. et al. Ultraconcentrated sodium bis(fluorosulfonyl)imide-based electrolytes for high-performance sodium metal batteries. *ACS Appl. Mater. Interfaces* **9**, 3723–3732 (2017).
20. Elia, G. A., Hoeppner, K. & Hahn, R. Comparison of chloroaluminate melts for aluminium graphite dual-ion battery application. *Batter. Supercaps* **4**, 368–373 (2021).
21. Rajput, N. N., Qu, X., Sa, N., Burrell, A. K. & Persson, K. A. The coupling between stability and ion pair formation in magnesium electrolytes from first-principles quantum mechanics and classical molecular dynamics. *J. Am. Chem. Soc.* **137**, 3411–3420 (2015).
22. Miao, L. et al. Aqueous electrolytes with hydrophobic organic cosolvents for stabilizing zinc metal anodes. *ACS Nano* **16**, 9667–9678 (2022).
This literature reports the use of a hydrophobic diethyl carbonate (DEC) with a low dielectric constant as a co-solvent for 2 M $Zn(SO_3CF_3)$ aqueous electrolyte. The preferential adsorption of DEC molecules onto the zinc metal anode surface to create a water-poor electrical double layer is demonstrated, which contributes to the suppressed hydrogen evolution.
23. Li, Z., Fuhr, O., Fichtner, M. & Zhao-Karger, Z. Towards stable and efficient electrolytes for room-temperature rechargeable calcium batteries. *Energy Environ. Sci.* **12**, 3496–3501 (2019).
24. Li, S. et al. Customized electrolyte and host structures enabling high-energy-density anode-free potassium-metal batteries. *ACS Energy Lett.* **8**, 3467–3475 (2023).
25. Zheng, J. et al. Extremely stable sodium metal batteries enabled by localized high-concentration electrolytes. *ACS Energy Lett.* **3**, 315–321 (2018).
This literature reports an early example of the use of low-viscosity, non-solvating hydrofluoroether co-solvents in the construction of localized high-concentration electrolytes for sodium metal batteries.
26. Hu, L. et al. Restructuring electrolyte solvation by a versatile diluent toward beyond 99.9% Coulombic efficiency of sodium plating/stripping at ultralow temperatures. *Adv. Mater.* **36**, 2312161 (2024).
A cyclic ether co-solvent with weaker solvating ability than the original linear ether solvent in the low-concentration $NaPF_6$ electrolyte is demonstrated, enhancing the coordination between Na^+ and anion, which leads to preferentially anion-derived solid electrolyte interphase and promotes reversibility of sodium plating and stripping.
27. Xu, C., Diemant, T., Liu, X. & Passerini, S. Locally concentrated deep eutectic liquids electrolytes for low-polarization aluminum metal batteries. *Adv. Mater.* **36**, 2400263 (2024).

28. You, C. et al. An inexpensive electrolyte with double-site hydrogen bonding and a regulated Zn^{2+} solvation structure for aqueous Zn-ion batteries capable of high-rate and ultra-long low-temperature operation. *Energy Environ. Sci.* **16**, 5096–5107 (2023).
Formamide with a high dielectric constant is adopted as a co-solvent for low-cost zinc acetate aqueous electrolytes, which coordinate with Zn^{2+} reducing water in the metal ion solvation sheath. It also reorganizes the hydrogen-bonded network and modifies the morphology of zinc metal anode through surface adsorption.
29. Hou, S. et al. Solvation sheath reorganization enables divalent metal batteries with fast interfacial charge transfer kinetics. *Science* **374**, 172–178 (2021).
A family of methoxyethyl-amine co-solvents exhibiting stronger coordination ability than the original 1,2-dimethoxyethane (DME) solvent towards Mg^{2+} is reported as co-solvents for non-aqueous magnesium metal batteries. The co-solvent replaces DME in the solvation sheath of Mg^{2+}, leading to reduced polarization and considerably promoting magnesium stripping and plating reversibility.
30. Xu, K. Nonaqueous liquid electrolytes for lithium-based rechargeable batteries. *Chem. Rev.* **104**, 4303–4417 (2004).
31. Fong, R., von Sacken, U. & Dahn, J. R. Studies of lithium intercalation into carbons using nonaqueous electrochemical cells. *J. Electrochem. Soc.* **137**, 2009–2013 (1990).
32. Guyomard, D. & Tarascon, J. M. Rechargeable $Li_{1+x}Mn_2O_4$/carbon cells with a new electrolyte composition: potentiostatic studies and application to practical cells. *J. Electrochem. Soc.* **140**, 3071–3081 (1993).
33. Geysens, P. et al. Solvation structure of sodium bis(fluorosulfonyl)imide-glyme solvate ionic liquids and its influence on cycling of Na-MNC cathodes. *J. Phys. Chem. B* **122**, 275–289 (2018).
34. Cao, R. et al. Enabling room temperature sodium metal batteries. *Nano Energy* **30**, 825–830 (2016).
35. Schafzahl, L., Hanzu, I., Wilkening, M. & Freunberger, S. A. An electrolyte for reversible cycling of sodium metal and intercalation compounds. *ChemSusChem* **10**, 401–408 (2017).
36. Wang, Y. et al. Enhanced sodium metal/electrolyte interface by a localized high-concentration electrolyte for sodium metal batteries: first-principles calculations and experimental studies. *ACS Appl. Energy Mater.* **4**, 7376–7384 (2021).
37. He, J., Bhargav, A., Shin, W. & Manthiram, A. Stable dendrite-free sodium-sulfur batteries enabled by a localized high-concentration electrolyte. *J. Am. Chem. Soc.* **143**, 20241–20248 (2021).
38. Guo, D., Wang, J., Lai, T., Henkelman, G. & Manthiram, A. Electrolytes with solvating inner sheath engineering for practical Na–S batteries. *Adv. Mater.* **35**, 2300841 (2023).
39. Chen, S. et al. High-voltage lithium-metal batteries enabled by localized high-concentration electrolytes. *Adv. Mater.* **30**, 1706102 (2018).
40. Cao, X., Jia, H., Xu, W. & Zhang, J.-G. Review — localized high-concentration electrolytes for lithium batteries. *J. Electrochem. Soc.* **168**, 010522 (2021).
41. Zhou, X. et al. Anion-reinforced solvation for a gradient inorganic-rich interphase enables high-rate and stable sodium batteries. *Angew. Chem. Int. Ed. Engl.* **61**, e202205045 (2022).
The addition of non-solvating co-solvents to high-concentration electrolytes is demonstrated, facilitating more anions to enter the solvation sheath of Na^+, which leads to an inorganic-rich solid electrolyte interphase and the improved performance.
42. Yi, Q. et al. Fluorinated ether based electrolyte enabling sodium-metal batteries with exceptional cycling stability. *ACS Appl. Mater. Interfaces* **11**, 46965–46972 (2019).
43. Zheng, X. et al. Bridging the immiscibility of an all-fluoride fire extinguishant with highly-fluorinated electrolytes toward safe sodium metal batteries. *Energy Environ. Sci.* **13**, 1788–1798 (2020).
44. Seh, Z. W., Sun, J., Sun, Y. & Cui, Y. A highly reversible room-temperature sodium metal anode. *ACS Cent. Sci.* **1**, 449–455 (2015).
45. Wang, S. et al. Stable sodium metal batteries via manipulation of electrolyte solvation structure. *Small Methods* **4**, 1900856 (2020).
46. Thenuwara, A. C. et al. Enabling highly reversible sodium metal cycling across a wide temperature range with dual-salt electrolytes. *J. Mater. Chem. A* **9**, 10992–11000 (2021).
47. Tomich, A. W. et al. A carboranyl electrolyte enabling highly reversible sodium metal anodes via a 'fluorine-free' SEI. *Angew. Chem. Int. Ed. Engl.* **61**, e202208158 (2022).
48. Doi, K. et al. Reversible sodium metal electrodes: is fluorine an essential interphasial component? *Angew. Chem. Int. Ed. Engl.* **58**, 8024–8028 (2019).
49. Li, Y. et al. Ultralow-concentration electrolyte for Na-ion batteries. *ACS Energy Lett.* **5**, 1156–1158 (2020).
50. Yamada, Y., Wang, J., Ko, S., Watanabe, E. & Yamada, A. Advances and issues in developing salt-concentrated battery electrolytes. *Nat. Energy* **4**, 269–280 (2019).
51. Zhou, J. et al. Low-temperature and high-rate sodium metal batteries enabled by electrolyte chemistry. *Energy Storage Mater.* **50**, 47–54 (2022).
52. Wang, C. et al. Extending the low-temperature operation of sodium metal batteries combining linear and cyclic ether-based electrolyte solutions. *Nat. Commun.* **13**, 4934 (2022).
53. Wang, Z. et al. Promoting fast Na ion transport at low temperatures for sodium metal batteries. *ACS Appl. Mater. Interfaces* **14**, 40985–40991 (2022).
54. Holoubek, J. et al. Tailoring electrolyte solvation for Li metal batteries cycled at ultra-low temperature. *Nat. Energy* **6**, 303–313 (2021).
55. Guo, D. et al. Low-temperature sodium–sulfur batteries enabled by ionic liquid in localized high concentration electrolytes. *Adv. Funct. Mater.* **34**, 2409494 (2024).
56. Xiao, N., Gourdin, G. & Wu, Y. Simultaneous stabilization of potassium metal and superoxide in K–O_2 batteries on the basis of electrolyte reactivity. *Angew. Chem. Int. Ed. Engl.* **57**, 10864–10867 (2018).
57. Liu, Q. et al. An ultra-low concentration electrolyte with fluorine-free bulky anions for stable potassium metal batteries. *Nano Res.* **16**, 8290–8296 (2023).
58. Zhang, F. et al. Weakly solvated electrolyte driven anion interface chemistry for potassium batteries/hybrid capacitors. *ACS Energy Lett.* **8**, 4895–4902 (2023).
59. Yu, Z. et al. Designing electrolytes with steric hindrance and film-forming booster for high-voltage potassium metal batteries. *Adv. Funct. Mater.* **34**, 2315446 (2024).
60. Xiao, N., McCulloch, W. D. & Wu, Y. Reversible dendrite-free potassium plating and stripping electrochemistry for potassium secondary batteries. *J. Am. Chem. Soc.* **139**, 9475–9478 (2017).
61. Liu, S. et al. An intrinsically non-flammable electrolyte for high-performance potassium batteries. *Angew. Chem. Int. Ed. Engl.* **59**, 3638–3644 (2020).
62. Chen, J. et al. Low-temperature high-areal-capacity rechargeable potassium-metal batteries. *Adv. Mater.* **34**, 2205678 (2022).
63. Chen, C. et al. Regulating the solvation structure of potassium ions using a multidentate ether in potassium metal batteries. *ACS Appl. Energy Mater.* **5**, 10366–10374 (2022).
64. Yi, X. et al. Safe electrolyte for long-cycling alkali-ion batteries. *Nat. Sustain.* **7**, 326–337 (2024).
65. Chen, X. et al. Phase transfer-mediated degradation of ether-based localized high-concentration electrolytes in alkali metal batteries. *Angew. Chem. Int. Ed. Engl.* **61**, e202207018 (2022).
The chemical degradation occurring between the ether-based localized high-concentration electrolytes and alkali metals is demonstrated, which is accelerated going from lithium to sodium, and particularly potassium, owing to their increasing trend to generate metal anions in a dynamic equilibrium with solvated electrons.
66. Chen, X., Meng, Y., Xiao, D., Wu, Y. & Qin, L. Tunning solvation structure in non-flammable, localized high-concentration electrolytes with enhanced stability towards all aluminum substrate-based K batteries. *Energy Storage Mater.* **61**, 102923 (2023).
67. Gao, P. et al. Ultrastable dendrite-free potassium metal batteries enabled by weakly-solvated electrolyte. *ACS Nano* **17**, 20325–20333 (2023).
68. Elia, G. A. et al. An overview and future perspectives of aluminum batteries. *Adv. Mater.* **28**, 7564–7579 (2016).
69. Meng, J. et al. Rapid-charging aluminium–sulfur batteries operated at 85 °C with a quaternary molten salt electrolyte. *Nat. Commun.* **15**, 596 (2024).
70. Pang, Q. et al. Fast-charging aluminium–chalcogen batteries resistant to dendritic shorting. *Nature* **608**, 704–711 (2022).
71. Lin, M. C. et al. An ultrafast rechargeable aluminium-ion battery. *Nature* **520**, 325–328 (2015).
72. Jiao, H., Wang, C., Tu, J., Tian, D. & Jiao, S. A rechargeable Al-ion battery: Al/molten $AlCl_3$-urea/graphite. *Chem. Commun.* **53**, 2331–2334 (2017).
73. Angell, M. et al. High Coulombic efficiency aluminum-ion battery using an $AlCl_3$–urea ionic liquid analog electrolyte. *Proc. Natl Acad. Sci. USA* **114**, 834–839 (2017).
74. Abood, H. M. A., Abbott, A. P., Ballantyne, A. D. & Ryder, K. S. Do all ionic liquids need organic cations? Characterisation of $[AlCl_2{\cdot}n\text{Amide}]^+$ $AlCl_4^-$ and comparison with imidazolium based systems. *Chem. Commun.* **47**, 3523–3525 (2011).
75. Xu, C. et al. Locally concentrated ionic liquid electrolytes for wide-temperature-range aluminum–sulfur batteries. *Angew. Chem. Int. Ed. Engl.* **63**, e202318204 (2024).
The addition of non-solvating co-solvent can effectively promote the fluidity and ionic conductivity without affecting the $AlCl_4^-/Al_2Cl_7^-$ equilibrium of the electrolyte, which promotes the kinetics of aluminium stripping and plating.
76. Liebenow, C. Reversibility of electrochemical magnesium deposition from Grignard solutions. *J. Appl. Electrochem.* **27**, 221–225 (1997).
77. Aurbach, D. et al. Prototype systems for rechargeable magnesium batteries. *Nature* **407**, 724–727 (2000).
78. Mizrahi, O. et al. Electrolyte solutions with a wide electrochemical window for rechargeable magnesium batteries. *J. Electrochem. Soc.* **155**, A103 (2008).
79. Zhao, W. et al. Chloride-free electrolytes for high-voltage magnesium metal batteries: challenges, strategies, and perspectives. *Chem. Eur. J.* **29**, e202203334 (2023).
80. Ding, M. S., Diemant, T., Behm, R. J., Passerini, S. & Giffin, G. A. Dendrite growth in Mg metal cells containing $Mg(TFSI)_2$/glyme electrolytes. *J. Electrochem. Soc.* **165**, A1983–A1990 (2018).
81. Zhao, W. et al. Tailoring coordination in conventional ether-based electrolytes for reversible magnesium-metal anodes. *Angew. Chem. Int. Ed. Engl.* **61**, e202205187 (2022).
Trimethyl phosphate, partially replacing 1,2-dimethoxyethane (DME) molecules in the solvation sheath of Mg^{2+}, is adopted as co-solvent for the $Ca(TFSI)_2$–DME electrolyte, which promotes the de-solvation kinetics and modifies solid electrolyte interphase for magnesium metal anodes with reduced polarization.
82. Wang, F. et al. Solvent molecule design enables excellent charge transfer kinetics for a magnesium metal anode. *ACS Energy Lett.* **8**, 780–789 (2023).
83. Bakulin, I. K. & Orekhov, M. A. Effect of long range interactions on the reduction of divalent ions in N,O-chelating solvents. *Phys. Chem. Chem. Phys.* **25**, 20686–20692 (2023).
84. Du, Y. et al. Strong solvent coordination effect inducing gradient solid-electrolyte-interphase formation for highly efficient Mg plating/stripping. *Energy Storage Mater.* **62**, 102939 (2023).
This literature replaces the previously adopted $Mg(TFSI)_2$ salt with a cheaper one, such as $Mg(SO_3CF_3)$, and clarifies the relationship between the solvation sheath in the electrolyte and the solid electrolyte interphase structure on magnesium metal anodes.

85. Zhang, D. et al. Constructing efficient $Mg(CF_3SO_3)_2$ electrolyte via tailoring solvation and interface chemistry for high-performance rechargeable magnesium batteries. *Adv. Energy Mater.* **13**, 2301795 (2023).
86. Wang, M. et al. Synergy between the coordination and trace ionization of co-solvents enables reversible magnesium electroplating/stripping behavior. *Energy Environ. Sci.* **17**, 630–641 (2023).
A trace ionization of amine and ether co-solvents is proposed, which leads to the formation of protonated molecules. These species promote the formation of MgH_2 in the solid electrolyte interphase and chemically associate with the $TFSI^-$ to neutrally charged ion pairs, which mitigate the migration and decomposition of $TFSI^-$ anion on magnesium metal anode and, therefore, promote the reversibility.
87. Fan, S. et al. A simple halogen-free magnesium electrolyte for reversible magnesium deposition through cosolvent assistance. *ACS Appl. Mater. Interfaces* **12**, 10252–10260 (2020).
88. Aurbach, D., Skaletsky, R. & Gofer, Y. The electrochemical behavior of calcium electrodes in a few organic electrolytes. *J. Electrochem. Soc.* **138**, 3536–3545 (1991).
89. Ponrouch, A., Frontera, C., Bardé, F. & Palacín, M. R. Towards a calcium-based rechargeable battery. *Nat. Mater.* **15**, 169–172 (2016).
90. Wang, D. et al. Plating and stripping calcium in an organic electrolyte. *Nat. Mater.* **17**, 16–20 (2018).
91. Kisu, K. et al. Monocarborane cluster as a stable fluorine-free calcium battery electrolyte. *Sci. Rep.* **11**, 7563 (2021).
92. Shyamsunder, A., Blanc, L. E., Assoud, A. & Nazar, L. F. Reversible calcium plating and stripping at room temperature using a borate salt. *ACS Energy Lett.* **4**, 2271–2276 (2019).
93. Hou, Z. et al. Correlation between electrolyte chemistry and solid electrolyte interphase for reversible Ca metal anodes. *Angew. Chem. Int. Ed. Engl.* **61**, e202214796 (2022).
94. Ye, L. et al. A rechargeable calcium–oxygen battery that operates at room temperature. *Nature* **626**, 313–318 (2024).
Dimethyl sulfoxide as a solvating co-solvent for an ionic liquid electrolyte using $Ca(TFSI)_2$ as salt and $EmimBF_4$ ionic liquid as solvent, which facilitates both the kinetics and reversibility of calcium metal anodes.
95. Dong, Y. et al. Dissolution, solvation and diffusion in low-temperature zinc electrolyte design. *Nat. Rev. Chem.* **9**, 102–117 (2025).
96. Luo, J. Y. & Xia, Y. Y. Aqueous lithium-ion battery $LiTi_2(PO_4)_3/LiMn_2O_4$ with high power and energy densities as well as superior cycling stability. *Adv. Funct. Mater.* **17**, 3877–3884 (2007).
97. Pang, G. et al. Enhanced performance of aqueous sodium-ion batteries using electrodes based on the $NaTi_2(PO_4)_3$/MWNTs-$Na_{0.44}MnO_2$ System. *Energy Technol.* **2**, 705–712 (2014).
98. Ming, J., Guo, J., Xia, C., Wang, W. & Alshareef, H. N. Zinc-ion batteries: materials, mechanisms, and applications. *Mater. Sci. Eng. R.* **135**, 58–84 (2019).
99. Dong, Y. et al. Non-concentrated aqueous electrolytes with organic solvent additives for stable zinc batteries. *Chem. Sci.* **12**, 5843–5852 (2021).
100. Ming, F. et al. Co-solvent electrolyte engineering for stable anode-free zinc metal batteries. *J. Am. Chem. Soc.* **144**, 7160–7170 (2022).
101. Li, Z. et al. A co-solvent in aqueous electrolyte towards ultralong-life rechargeable zinc-ion batteries. *Energy Storage Mater.* **56**, 174–182 (2023).
102. Dong, Y. et al. Cell-nucleus structured electrolyte for low-temperature aqueous zinc batteries. *J. Energy Chem.* **83**, 324–332 (2023).
When the content of 1,2-dimethoxyethane is not higher than 30%, it does not replace water in the solvation sheath of Zn^{2+} but pushes more anions to enter the Zn^{2+} solvation, which results in the formation of inorganic-rich solid electrolyte interphase on zinc metal anodes.
103. Guan, K. et al. A dual salt/dual solvent electrolyte enables ultrahigh utilization of zinc metal anode for aqueous batteries. *Adv. Mater.* **36**, 2405889 (2024).
104. Cao, L. et al. Solvation structure design for aqueous Zn metal batteries. *J. Am. Chem. Soc.* **142**, 21404–21409 (2020).
105. Hao, J. et al. Boosting zinc electrode reversibility in aqueous electrolytes by using low-cost antisolvents. *Angew. Chem. Int. Ed. Engl.* **60**, 7366–7375 (2021).
106. Wang, Y. et al. Sulfolane-containing aqueous electrolyte solutions for producing efficient ampere-hour-level zinc metal battery pouch cells. *Nat. Commun.* **14**, 1828 (2023).
Sulfolane is adopted as an organic co-solvent for the 3 M $Zn(SO_3CF_3)_2$ aqueous electrolyte. The addition of sulfolane leads to the formation of a micelle structure, in which sulfolane molecules constrain water in nanodomains to hinder proton reduction on zinc metal anodes.
107. Feng, D. et al. Immunizing aqueous Zn batteries against dendrite formation and side reactions at various temperatures via electrolyte additives. *Small* **17**, 2103195 (2021).
108. Meng, C. et al. Multifunctional water–organic hybrid electrolyte for rechargeable zinc ions batteries. *Chem. Eng. J.* **450**, 138265 (2022).
109. Shi, X. et al. Metallic zinc anode working at 50 and 50 mAh cm^{-2} with high depth of discharge via electrical double layer reconstruction. *Adv. Funct. Mater.* **33**, 2211917 (2023).
110. Deng, W., Xu, Z. & Wang, X. High-donor electrolyte additive enabling stable aqueous zinc-ion batteries. *Energy Storage Mater.* **52**, 52–60 (2022).
111. Hao, Y. et al. Hybrid electrolyte engineering enables reversible Zn metal anodes at ultralow current densities. *J. Power Sources* **584**, 233631 (2023).
112. Zhang, T. et al. A solubility-limited, non-protonic polar small molecule co-solvent reveals additive selection in inorganic zinc salts. *Energy Storage Mater.* **65**, 103085 (2024).
113. Liu, S. et al. Monolithic phosphate interphase for highly reversible and stable Zn metal anode. *Angew. Chem. Int. Ed. Engl.* **62**, e202215600 (2023).
This literature demonstrates the positive effect of the solid electrolyte interphase generated in the presence of a dimethyl methylphosphonate co-solvent on the cyclability of zinc metal anodes in aqueous electrolytes.
114. Ma, Q. et al. Regulation of outer solvation shell toward superior low-temperature aqueous zinc-ion batteries. *Adv. Mater.* **34**, 2207344 (2022).
115. Han, J. et al. A thin and uniform fluoride-based artificial interphase for the zinc metal anode enabling reversible Zn/MnO_2 batteries. *ACS Energy Lett.* **6**, 3063–3071 (2021).
116. Li, T. C. et al. A universal additive strategy to reshape electrolyte solvation structure toward reversible Zn storage. *Adv. Energy Mater.* **12**, 2103231 (2022).
117. Jiang, W. et al. Breaking the trade-off between capacity and stability in vanadium-based zinc-ion batteries. *Chem. Sci.* **15**, 2601–2611 (2024).
118. Han, K. S. et al. Factors influencing preferential anion interactions during solvation of multivalent cations in ethereal solvents. *J. Phys. Chem. C* **125**, 6005–6012 (2021).
119. Sun, Q. et al. Dipole–dipole interaction induced electrolyte interfacial model to stabilize antimony anode for high-safety lithium-ion batteries. *ACS Energy Lett.* **7**, 3545–3556 (2022).
120. Liu, X. et al. Difluorobenzene-based locally concentrated ionic liquid electrolyte enabling stable cycling of lithium metal batteries with nickel-rich cathode. *Adv. Energy Mater.* **12**, 2200862 (2022).
121. Liu, X. et al. Locally concentrated ionic liquid electrolyte with partially solvating diluent for lithium/sulfurized polyacrylonitrile batteries. *Adv. Mater.* **34**, 2207155 (2022).
122. Liu, X. et al. PFAS-free locally concentrated ionic liquid electrolytes for lithium metal batteries. *ACS Energy Lett.* **9**, 3049–3057 (2024).
123. Liu, X. et al. Development of PFAS-free locally concentrated ionic liquid electrolytes for high-energy lithium and aluminium metal batteries. *Acc. Chem. Res.* **58**, 354–365 (2025).

Acknowledgements

Financial support from the Helmholtz Association, National Key R & D Program (2022YFB2404600), Natural Science Foundation of China (Key Project of 52131306), Project on Carbon Emission Peak and Neutrality of Jiangsu Province (BE2022031-4), the Start-up Research Fund of Southeast University (4003002418) and the Big Data Computing Center of Southeast University are acknowledged.

Author contributions

X.L. and S.P. conceived the idea. X.L. and X.D. read and summarized the relevant literature. X.L. and X.D. wrote the original draft. H.A. revised the original draft. Y.W. revised the original draft. S.P. revised the original draft, supervised the project and acquired the funding.

Competing interests

The authors declare no competing interests.

[1]School of Energy and Environment & Z Energy Storage Center, Southeast University, Nanjing, China. [2]Helmholtz Institute Ulm (HIU) Electrochemical Energy Storage, Ulm, Germany. [3]Karlsruhe Institute of Technology (KIT), Karlsruhe, Germany. [4]Department of Science and Engineering of Materials, Environment and Urban Planning, Marche Polytechnic University, Ancona, Italy. [5]Austrian Institute of Technology (AIT), Center for Transport Technologies, Wien, Austria. [6]These authors contributed equally: Xu Liu, Xu Dong.